Velocity and transport of the Makassar Strait throughflow

R. Dwi Susanto and Arnold L. Gordon

Lamont-Doherty Earth Observatory of Columbia University, Palisades, New York, USA

Received 9 April 2004; revised 27 August 2004; accepted 15 December 2004; published 26 January 2005.

[1] Analyses of ocean current measurements from two moorings in the Makassar Strait (MAK-1, December 1996 to July 1998, and MAK-2, December 1996 to February 1998) with newly processed acoustic Doppler current profiler (ADCP) data provide a new estimate of transport and vertical velocity structure for this important passageway of the Indonesian Throughflow. The 7-month record of the MAK-1 ADCP and the 3-month record of the MAK-2 ADCP, nominally set at depths of 150 m, are extrapolated to the end of the mooring period using a surface layer relationship to the shallowest current meter at 200 m and to the regional winds. The southward transport within Makassar Strait is confined for the most part to the upper 750 m, above the blocking topographic sill of Makassar Strait. The transport maximum occurs within the thermocline (100–300 m). After the temporal mean flow has been removed, the vertical structure of the along channel flow in the upper 750 m is decomposed using the empirical orthogonal function (EOF) method. The first two modes contain 91% of the total variance. For the entire mooring period, the total depth-integrated transport was 8.1 ± 1.5 Sv (Sv = 1×10^6 m^3/s), with 7.9 ± 1.2 Sv for calendar year1997. During the peak of 1997/1998 El Niño from September 1997 to mid-February 1998, the first mode time series displays northward flow, enhancing the vertical shear within the thermocline and reducing the mean throughflow to 4.6 ± 0.9 Sv.

Citation: Susanto, R. D., and A. L. Gordon (2005), Velocity and transport of the Makassar Strait throughflow, *J. Geophys. Res.*, *110*, C01005, doi:10.1029/2004JC002425.

1. Introduction

[2] As the westernmost deep channel of the inter-ocean routes within the Indonesian seas, Makassar Strait is expected to carry the bulk of the Indonesian Throughflow (ITF) [*Wajsowicz*, 1996]. Water mass analysis confirms that the Makassar Strait is the major path for the ITF from the equatorial Pacific en route to the various export passages of the Nusa Tenggara Islands arc (Lombok, Ombai, and Timor) to the eastern Indian Ocean (Figure 1) [*Gordon and Fine*, 1996].

[3] On 23 November 1996 the MAK-1 mooring was deployed at 2°52′S, 118°27′E, and MAK-2 was deployed at 2°51′S, 118°38′E, both within the Labani Channel, a 45-km-wide constriction of the Makassar Strait (at >50 m depth). Both MAK-1 and MAK-2 carried an upward looking acoustic Doppler current profiler (ADCP) at 150 m and five current meters at 200 m, 250 m, 350 m, 750 m, and 1500 m for MAK-1 and four current meters at 205 m, 255 m, 305, and 755 m for MAK-2 (Figure 2). The moorings included temperature and temperature-pressure sensors. In addition, in close proximity to the moorings, there were pressure-inverted echo sounders (PIES) [*Waworuntu et al.*, 2001]. In anticipation of mooring blowover, the ADCPs were set in the "surface tracking" mode and data can be corrected for the vertical oscillation; bin 1 is the closest to the ADCP sensor at 140 m depth while bin 25 is set at 52 m above the surface (8-m-depth bin increment). Hence ADCP still records water column data even though the blowover drags the instrument to 52 m below the setting depth (zero-wire angle).

[4] Estimates of the Makassar Strait transport based on two moorings have been presented [*Gordon and Susanto*, 1999; *Gordon et al.*, 1999; *Wajsowicz et al.*, 2003], but these estimates were hindered by the absence of a complete surface layer record from the ADCP. The MAK-2 ADCP time series spans only 3 months, late November 1996 to early March 1997, and the MAK-1 ADCP spanning a period of slightly over 7 months, from late November 1996 into July 1997. The MAK-1 ADCP record has only recently been processed, overcoming a compass recording problem. The objective of this paper is for the first time to apply empirical orthogonal function (EOF) method to the MAK time series in order to determine the vertical structure of the velocity profile and to provide an improved estimate of the throughflow within Makassar Strait.

[5] The outline of the paper is as follows. In section 2 the MAK ADCP time series is extrapolated to the end of the mooring period using a statistical relationship derived from the 7 months of data to the shallowest current meter at 200 m and to the regional winds. In section 3 the integrated velocity profile across the Makassar Strait at the Labani Channel constriction is then decomposed into vertical empirical modes and their temporal variability using EOF analysis. The transport estimates from the full depth velocity profiles

0148-0227/05/2004JC002425$09.00

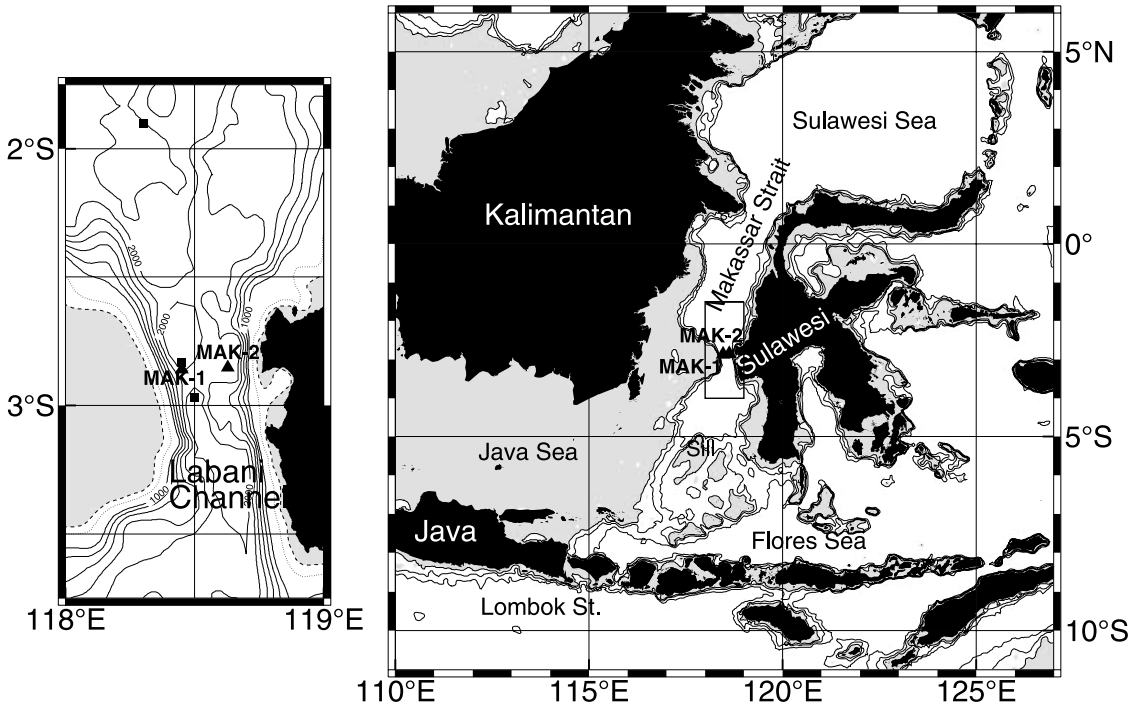

Figure 1. Map of the Makassar Strait and adjacent seas. The positions (triangles) of the MAK-1 (2°52′S, 118°27′E; from 23 November 1996 to 8 July 1998) and MAK-2 (2°51′S, 118°38′E; from 1 December 1996 to 21 February, 1998) moorings in the Makassar Strait are shown in the insert. The shaded area is less than 100 m.

and the upper 750 m EOF modes are discussed in section 4. Hereinafter, "mode" refers to EOF mode.

2. Along-Channel Vertical Velocity Profiles

2.1. Velocity Profiles From ADCPs and Current Meters

[6] Before combining the ADCP velocity for the surface layer and deeper current meter velocity time series, an adjustment of the velocity-pressure profile is needed to account for mooring blowover. As reported by *Susanto et al.* [2000] and *Ffield et al.* [2000], strong semidiurnal and diurnal tides with significant fortnightly modulation are the most dominant features of the current meter time series. The fortnightly amplitude is approximately 0.50 m/s. Histograms of the shallowest MAK-1 current meter (CM200) and the first two shallowest MAK-2 current meters indicate that during the entire record, 90% of MAK-1 CM200 data were obtained as the instrument fluctuated between 200 and 300 m depth, with a median at 238 m (Figure 3a). Meanwhile, 90% of the top MAK-2 current meter data were obtained as the instrument oscillated between 210 and 260 m depth, with a median at 223 m, and 32% of them were recorded at the zero-wire angle depth, 210 m (Figure 3b). The deeper current meter exhibited less excursion; 90% of the velocity data derived from CM of MAK-2 that set at 255 m were obtained as the instrument fluctuated between 260 and 310 m, and 35% of them were recorded at the zero-wire angle depth, 260 m (Figure 3c). The mooring blowover and velocity at the western side (MAK-1) were slightly higher than those at the eastern side (MAK-2). Because the ADCPs were attached to the same wire, 50 m above the shallowest current meter, they experienced commensurate blowover. ADCP velocity-pressure time series are adjusted and constructed based on data associate with their bin numbers. A 2-day low-passed filter was applied to both ADCP and current meter data to remove the semidiurnal and diurnal tides, and the data were decimated into daily data.

[7] The cross-correlation values of the upper three current meters within each mooring and between the two moorings are high. For example, the correlation of the 200-m and 250-m current meters of MAK-1 and MAK-2 is above 0.95. Meanwhile, the correlation between MAK-1 and MAK-2 at 350 m is 0.8. At 750 m, the cross-correlation value drops to 0.76. Higher speeds along the western side of Labani (MAK-1) than that in the east (MAK-2) indicate the presence of western intensification. When MAK-1 southward speed is larger than 0.15 m/s, the averaged MAK-2 southward speed is about 88% of MAK-1 speeds. Below 300 m the percentage is dropped to 75%. *Burnett et al.* [2000] regional model of the Indonesian seas (their Figure 1) shows that within Makassar Strait the southward flow is shifted toward the western boundary. In addition, the MAK moorings were sited within a constriction formed by a shallow bank jutting from the west (Figure 1), which may enhance the local western intensification.

[8] After blowover adjustment, the data are linearly interpolated with depth, in 10-m increments for each mooring. To combine the velocity profiles of the two moorings into an integrated velocity profile across the strait, we use two interpolation approaches offering reasonable upper and lower limits, respectively. For the upper limit estimate, the

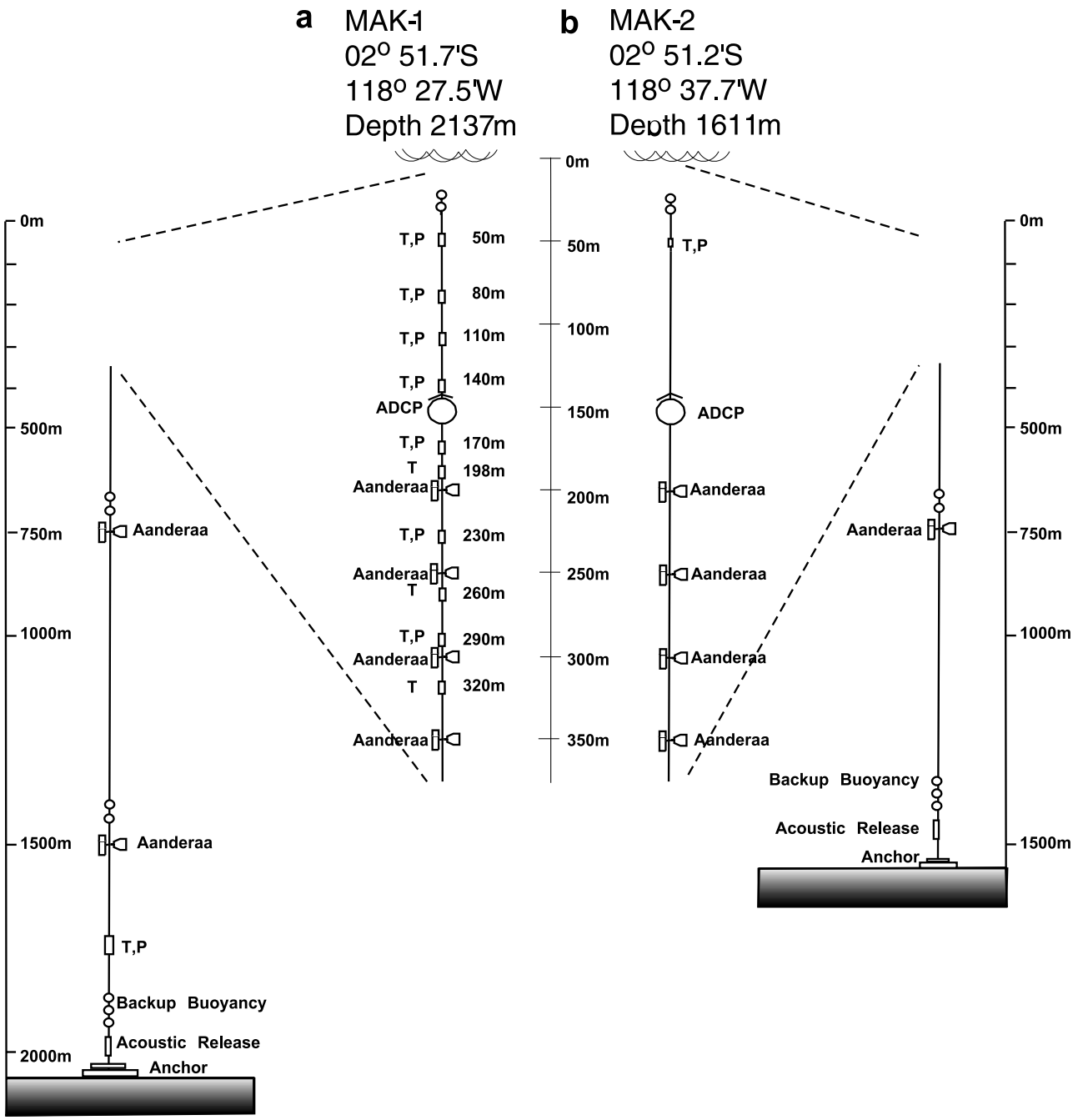

Figure 2. The configuration of (a) MAK-1 and (b) MAK-2. "T" shows the position of the T-pod temperature sensors, and "P" stands for pressure as measured at most of the T-pods. The ADCP is an upward looking RDI 300-Hz acoustical Doppler profiler.

linearly interpolated measured velocity data between the moorings are extrapolated to the channel walls. Also, we assume that the velocity below 1500 m is the same as the velocity observed at the 1500-m current meter. To compensate a possibility of higher velocity between MAK-1 and the western wall, when there are no MAK-2 velocity data, MAK-1 velocity data are used to represent the full channel. The resulting velocity profile is considered to represent the upper limit. For the lower limit estimate, zero values are set at the sidewalls of the channel (no slip at the walls and bottom) and with a quadratic interpolation between boundaries and the mooring lines. To take into account of the fact that MAK-1 velocity is higher than that of MAK-2, an appropriate scaling factor is estimated by regression analyses between MAK-1 and MAK-2 at each depth. When there are no MAK-2 velocity data, the velocity is estimated by multiplying the scaling factor to the MAK-1 velocity.

[9] As we have only two mooring positions monitored across the 45-km Labani channel, we do not know the entire cross-strait structure of the velocity profile. To approximate the full cross-channel transport, we will use

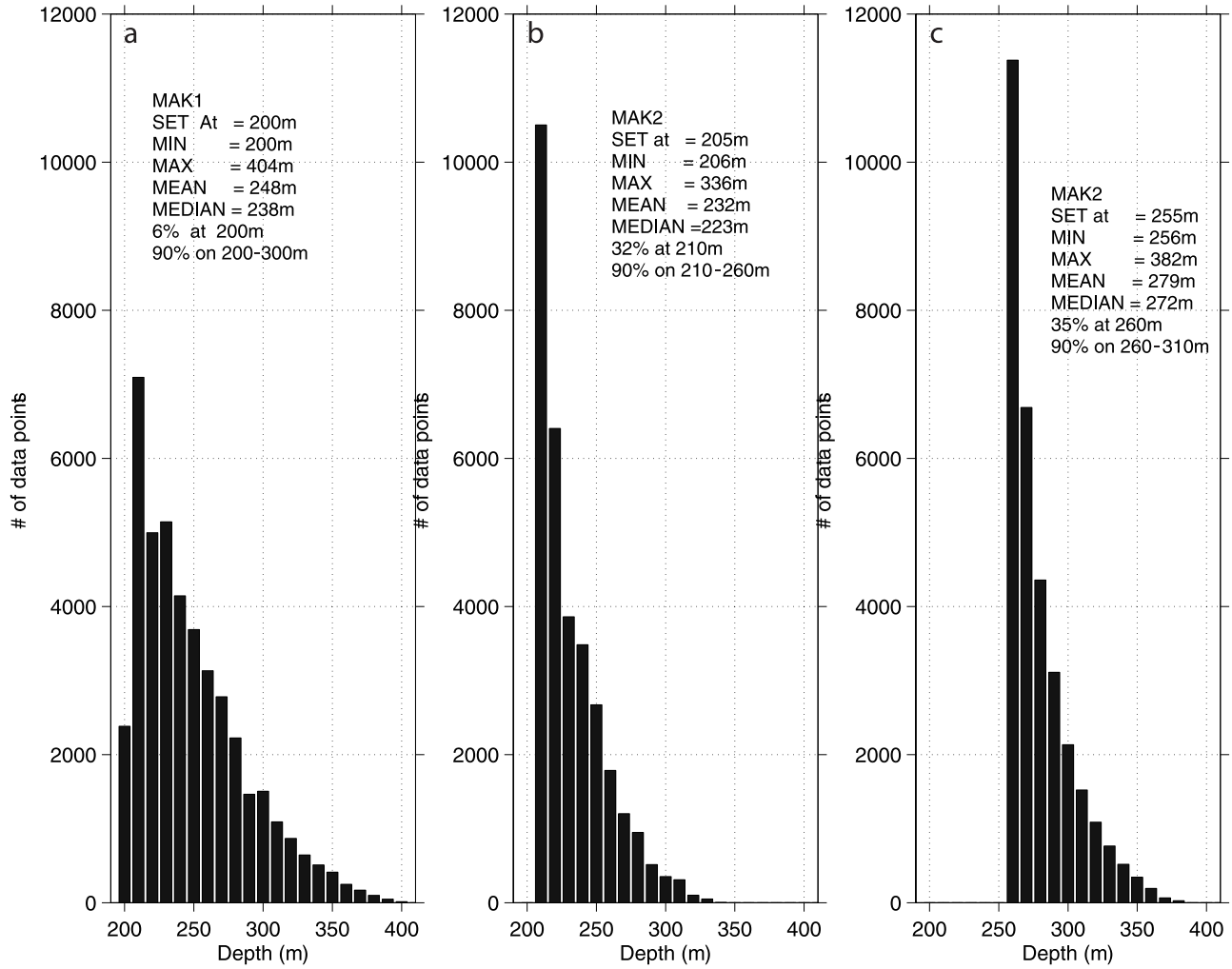

Figure 3. Histograms of the pressure (a) from the uppermost MAK-1 current meter, and (b, c) from the first two shallowest MAK-2 current meters.

the averaged value of both limits to represent the integrated velocity profile across the strait (Figure 4). A monthly low-pass filter has been applied to the data before contouring; however, for calculating the vertical structures and transports (discussed in the next section), no monthly low-pass filter is applied to the daily ADCP and current meter data.

2.2. Upper 200 m Velocity Estimates

[10] As noted above, the MAK-1 and MAK-2 ADCP surface layer data cover only the first 7 and 3 months of the total mooring duration. In order to determine the full transport, we must extrapolate the surface layer velocity to the end of the mooring period. To do so, we investigate the correlation between each bin of the observed ADCP time series with the shallowest current meter time series at 200 m (CM200). The correlation values between each bin of the ADCP time series and the CM200 remain high, above 0.8 for bin 1 to bin 13 (bin 1, at 140 m, is the closest bin to the ADCP instrument; Figure 5). MAK-1 ADCP, with the longer time series, shows high correlation values for all bins from bin 1 to 17. Meanwhile, MAK-2 ADCP shows a drop in correlation value after bin 13. We assume that the 7-month correlation between CM200 and ADCP holds for the entire 18-month mooring record, and then the ADCP time series of each bin from 1 to 13 is extrapolated for the entire mooring record. Again, regression analysis is used to find the appropriate scale when extrapolating the ADCP data. Though the ADCP covers only 7 months, from November to July, which may cause some bias in estimating the mean flow, the ADCP time series cover the peaks of both the northwest monsoon and the southeast monsoon. The scaling amplitude factor from the regression analysis may capture these monsoon effects and lessen the bias of the mean flow.

[11] The drop in correlation value between the CM200 and ADCP bin time series at and above bin 14 (bin 14 has an average depth of 60 m) is probably due to the fact that the upper 60 m velocity is affected by the regional winds. *Gordon et al.* [2003a] provide a concept linking the Makassar surface layer flow to the regional winds. They show that the zonal monsoon winds in the Java Sea (110°E to 118°E and 7°S to 4°S) correlate with the upper 60-m Makassar ADCP (bin 14 to 20) minus the CM200 time series, with a correlation coefficient of 0.8 and with the

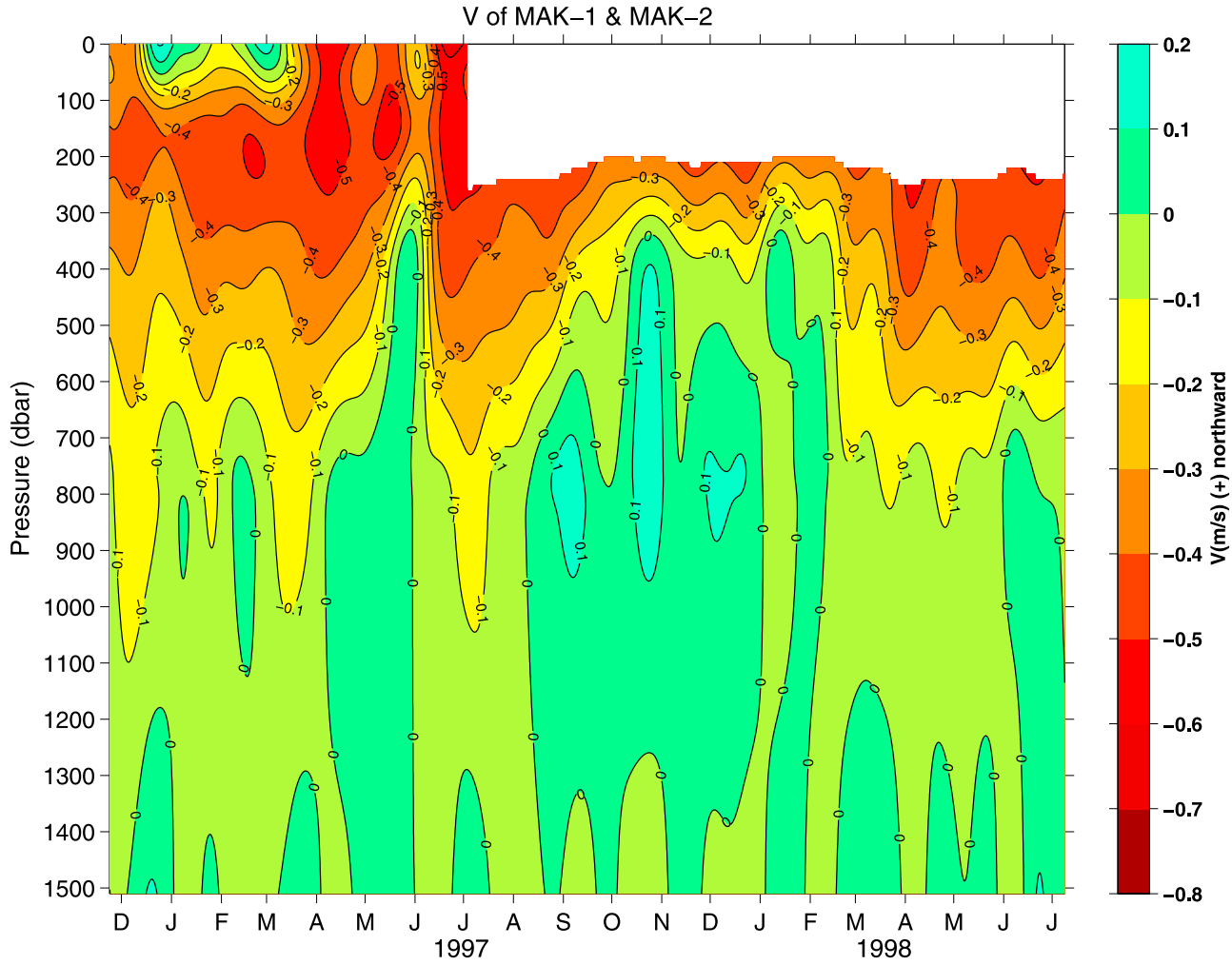

Figure 4. Integrated along-channel velocity profile across the Makassar Strait at the Labani channel constriction as derived from the ADCPs and current meter data of both moorings (MAK-1 and MAK-2). For clarity in presenting the figure, a monthly low-pass filter has been applied before contouring. The contour interval is 0.10 m/s. Negative values denote southward flow.

speeds lagged by 10 days to the Java winds. *Gordon et al.* [2003a] propose that this effect is a consequence of monsoon wind shifting of the low-salinity, buoyant, water of the shallow Java Seawater into (northern winter) and from (northern summer) the southern Makassar Strait, altering the meridional pressure gradient in the Makassar surface layer relative to the thermocline. Using this concept, we extrapolate the observed ADCP record of the upper 60 meters (bins 14 to 20 minus CM200 velocity) for the entire mooring period. The calculations are carried out for both moorings separately.

[12] On the basis of 7 months MAK-1 ADCP, the standard deviation of the difference between in situ ADCP measurement and synthetic data based on the zonal Java winds (for the top 60 m) and current meter at 200 m (in the lower 110 m) is calculated. The standard deviation varies from 0.11 m/s in the surface and 0.07 m/s in the deepest ADCP bin. Compared to the mean velocity of −0.47 m/s and maximum velocity of −0.82 m/s, the maximum standard deviation is less than 25% of the mean velocity. In addition, it is noted that the shallowest 15% (approximately 20 m) of the ADCP in situ measurements may be contaminated by sea surface scatter of the acoustical energy. With this error estimate, we are confident that our extrapolation of the 7 months ADCP time series provides a reasonable simulation of the actual velocity profile in the top 200 m for the entire mooring record.

[13] With a complete time series in the top layer, we now combine the extended surface layer velocity with the velocity data derived from all the current meter time series for each mooring. Using the upper and lower limits in the interpolation between moorings as described above, the integrated velocity across the strait is shown in Figure 6.

3. Vertical Mode Structure

[14] Before inspecting the composite MAK-1 and MAK-2 along-channel velocity profile, we compare those two profiles during their common recording period from 1 December 1996 to February 1997. The temporal mean flow indicated southward flow with MAK-1 velocity was larger than that of MAK-2. The surface velocity of MAK-1 was

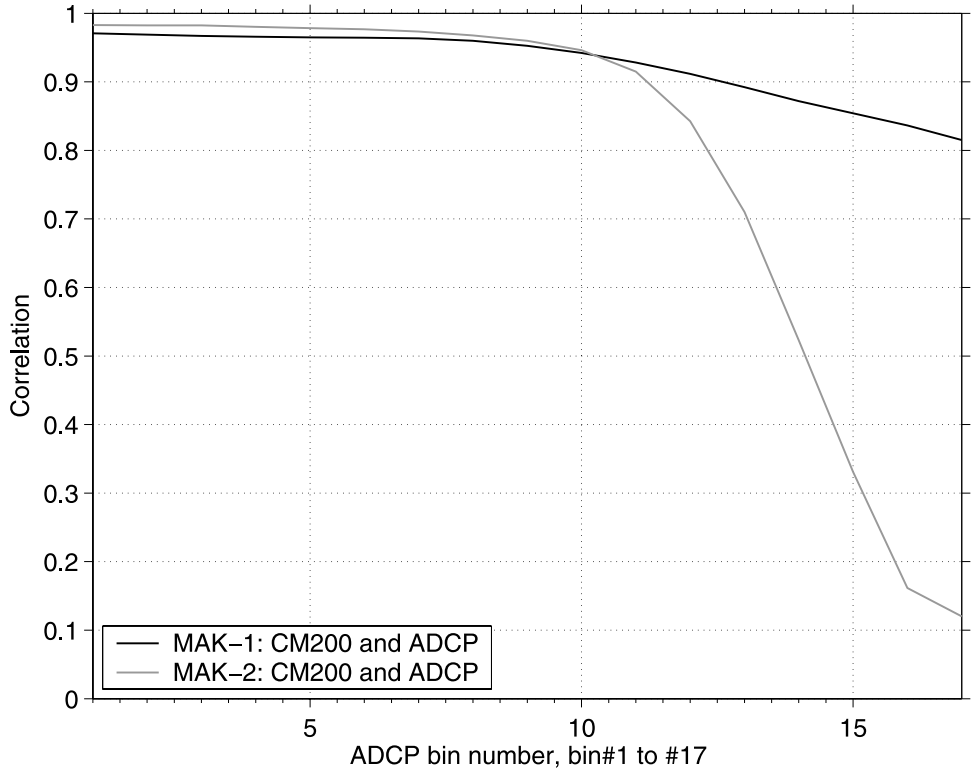

Figure 5. Correlation values between each bin of the ADCP velocity time series and the shallowest current meter (at a nominal of 200 m) for each mooring. Upward looking ADCPs attached to both the MAK-1 and MAK-2 moorings at 150 m depth (zero wire angle) contain 25 bins with an increment of 8 m. Bin 1 is at 140 m, the closest to the ADCP sensor, while bin 25 is set at 52 m above the surface (for the zero blowover condition).

−0.35 m/s (southward) with a maximum velocity at 150 m reached −0.56 m/s. MAK-2 surface velocity was −0.22 m/s with a maximum velocity at 190 m reached −0.42 m/s.

[15] From the integrated velocity profile across the strait of both moorings, the temporal mean velocity below 750 m was less than 0.02 m/s, indicating that the bulk of the throughflow, as expected, occurs above the Makassar sill depth of approximately 680 m [*Gordon et al.*, 2003b]. For the entire mooring record, the bulk throughflow was always southward. The high-resolution (11 km in the horizontal and 54 levels in the vertical) global ocean circulation model from the Japanese Earth Simulator shows a similar result, with strong southward flow including a maximum within the thermocline [*International Pacific Research Center* (*IPRC*), 2004].

[16] Because most of the throughflow resides in the upper 750 m and both moorings have a current meter at 750 m, the EOF analysis of the integrated velocity profile is only performed up to this depth. Before applying the EOF analysis, the temporal mean velocity profile (solid black line in Figure 7) has been removed. The surface velocity of the mean flow is −0.35 m/s; there is a maximum flow of −0.43 m/s at 160 m.

[17] The EOF analysis shows that only the first two modes are significant, with the first mode accounting for 68.7% of the variance and the second mode accounting for 21.9% of the variance (Figure 7). The first mode is characterized by a gradual decay of surface flow to nearly zero around 150 m, gradually increasing to maximum 0.13 m/s at 400 m, and a gradual decay below this depth. The second mode is characterized by a surface intensification flow that decays to zero around 340 m and flow that is of opposite direction below this depth.

[18] During the peak of 1997/1998 El Niño from September 1997 to February 1998, the first mode of variability is negative, indicating a northward anomaly, reducing the southward mean flow, while enhancing the vertical shear velocity within the thermocline. Northward anomaly also occurs during the intrusion of Kelvin wave in May 1997 [*Sprintall et al.*, 2000]. For the rest of the record, the first mode variability is positive, signifying an enhancement of the mean southward flow. Though a longer time series is needed to confirm this, we suggest that the first mode variability is a consequence of remote forcing, i.e., the 1997/1998 El Niño and Kelvin waves. The entire water column above the sill depth is affected, rather than confined to the surface layer as seen in EOF analysis of large-scale numerical model data [*Potemra et al.*, 2003]. This discrepancy may be due to the fact that their numerical model upper transport estimate was also stronger during 1997/1998 El Niño (opposite to our mooring measurement data). Part of this discrepancy may be due to the location of the model transect farther north of equator [*Potemra et al.*, 2003], and the resolution of the model could not fully resolve the complex geometry of Indonesian Seas [*IPRC*, 2004].

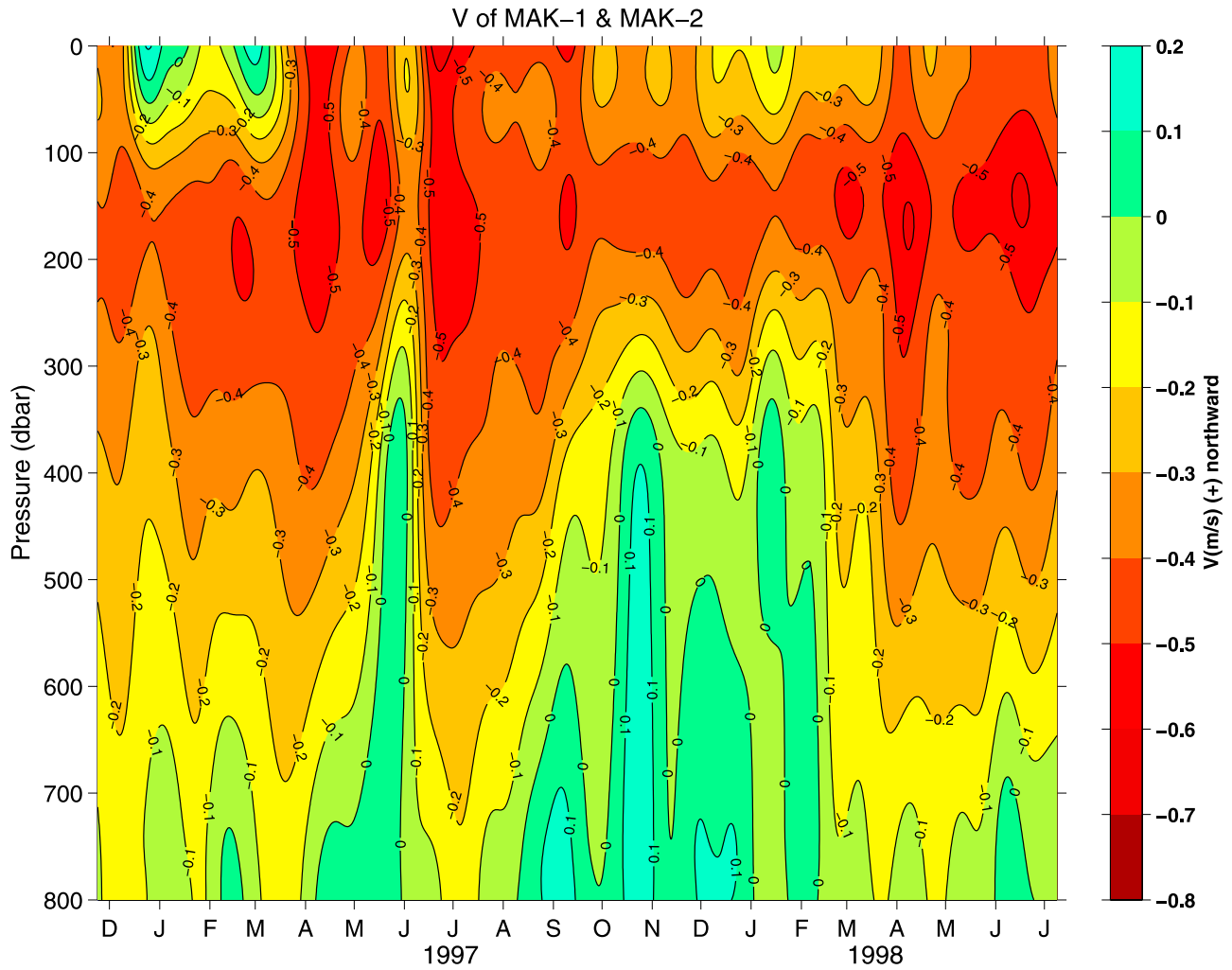

Figure 6. Integrated along-channel velocity profile across the strait derived from the ADCPs and current meter data of both moorings (MAK-1 and MAK-2). The ADCP time series were extrapolated beyond the length of the records using regression analyses between each ADCP bin time series and the shallowest current meter, and zonal wind speeds in the Java Sea, as explained in the text.

[19] The surface intensified flow of the second mode is probably associated with regional monsoonal winds. During the northwest monsoon, strong northward flows inhibited the mean southward throughflow. On the other hand, southward flow was observed during the southeast monsoon, enhancing the mean throughflow. As expected, weaker northward flow during the winter 1997/1998 results from anomalously easterly winds during the peak of 1997/98 El Niño in the Java Sea region [*Saji et al.*, 1999]. In addition, the easterly in the Java Sea region also caused coastal upwelling south of Sumatra-Java during the 1997/1998 El Niño –Southern Oscillation (ENSO)-Indian Ocean Dipole event [*Murtugudde et al.*, 2000], as observed from frequently repeated XBT temperature section [*Feng and Meyers*, 2003], SST, and sea level [*Susanto et al.*, 2001].

4. Makassar Volume Transport

[20] Using the same Makassar cross-section bathymetry as used by *Gordon and Susanto* [1999] and *Gordon et al.* [1999], which were derived from ship echo sounder and *Smith and Sandwell* [1997] bathymetry, the integrated volume transport time series for the EOF modes can be calculated by multiplying the vertical mode structure with its temporal mode and the Makassar cross-sectional area. Estimates of the Makassar Strait throughflow transport using the MAK time series data are summarized in Table 1 (positive values indicate southward transport from the Pacific Ocean to the Indian Ocean).

Table 1. Estimates of Depth-Integrated Transport in the Makassar Strait for the 1997 Calendar Year[a]

	Range (Sv; 1 Sv = 10^6 m^3/s)	1997 Mean (Sv)
Gordon and Susanto [1999]	6.7–11.0	9.3
Gordon et al. [1999]	6.7–11.3	9.2
Vranes et al. [2002][b]	6.9–10.8	8.9
Wajsowicz et al. [2003]	4.7–16.0	6.4
This study	6.7–9.1	7.9 ± 1.2

[a]Positive values are associated with southward transports from the Pacific Ocean to the Indian Ocean.
[b]Only using the top 700 m MAK-1 time series.

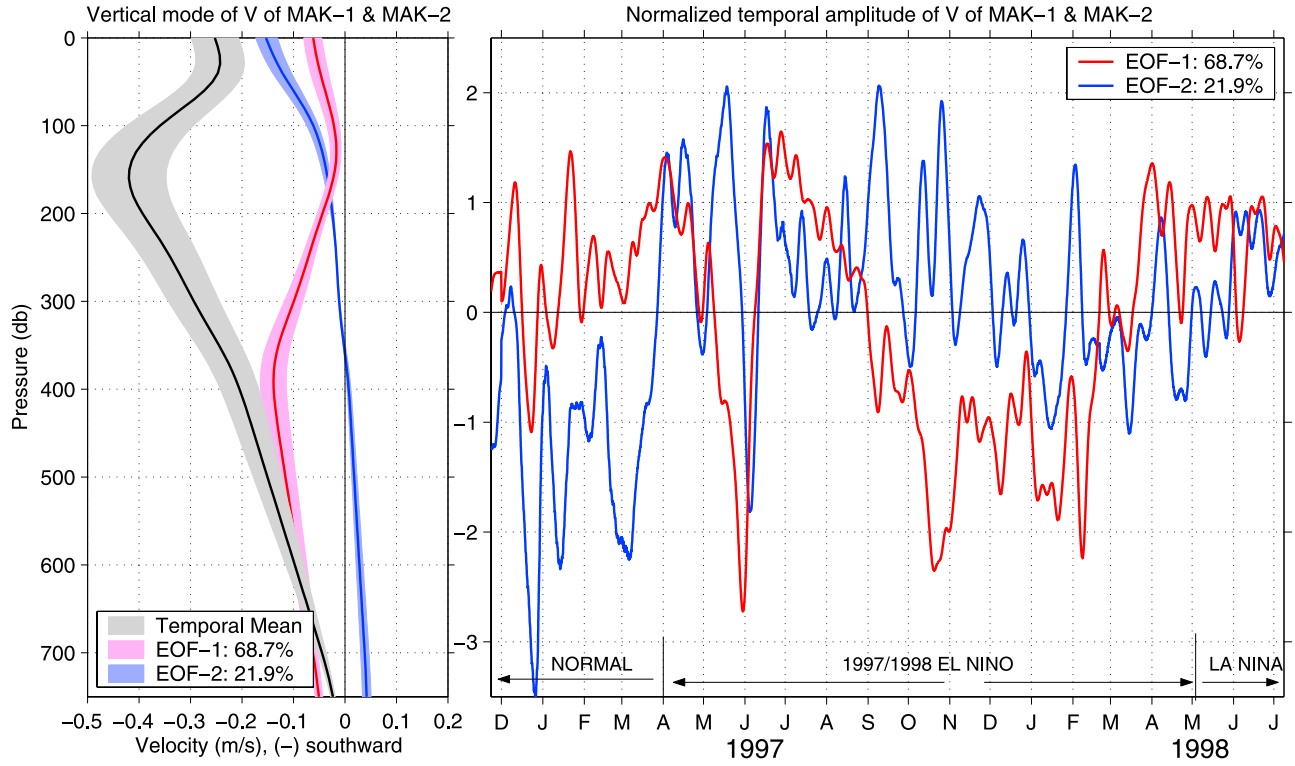

Figure 7. Vertical mode structures and their time series derived from empirical orthogonal function (EOF) analysis on the integrated velocity profile across the strait of MAK-1 and MAK-2 (Figure 6). Black line shows the along-channel mean flow. The red and blue lines are the first two EOF modes, respectively. Shaded area in the vertical structures indicates the upper and lower limits of velocity interpolation across the strait.

[21] The mean value of the total integrated transport (black line in Figure 8) during the MAK deployment period was 8.1 ± 1.5 Sv, and for the calendar year 1997, the transport was 7.9 ± 1.2 Sv. The new transport estimate differs somewhat from previous estimates. For comparison, *Gordon and Susanto* [1999] and *Gordon et al.* [1999] used four simple profiles to capture four possibilities: maximum, minimum, average, and seasonal dependence (the latter was offered as the most realistic profile) of velocities above the shallowest current meter at 200 m, as suggested by the MAK-2 ADCP and model results. The estimated 1997 calendar total transport for the four profiles were: 11.3 Sv, 9.4 Sv, 6.7 Sv, and 9.2 Sv, respectively. Using monthly data, the normal mode based treatment of *Wajsowicz et al.* [2003] yields a calendar 1997 of 6.4 Sv with a upper and lower bound of 16.0 and 4.7 Sv. Much of the differences can probably be explained by our use of the full 7-month record from the MAK-1 ADCP, and by extrapolation of the surface layer speeds to the period of no ADCP data using a surface layer relationship to the shallowest current meter at 200 m and to the regional winds.

[22] Though longer time series are needed, the presence of interannual modulation associated with 1997/1998 El Niño event over intraseasonal and seasonal frequencies is clearly seen. As in the ITF outflow passages, the 1997/1998 El Niño event seems to almost completely suppress the annual cycle [*Hautala et al.*, 2001]. The total transport varies from 0.6 Sv in late May 1996 to 14.7 Sv in June and July 1997. During the peak of 1997/1998 El Niño phase from September 1997 to February 1998, the first EOF mode gave northward transport, reducing the mean southward transport to 4.6 ± 0.9 Sv.

5. Summary

[23] The vertical velocity profile and the depth-integrated transport across the Makassar Strait at the Labani channel constriction are estimated based on analyses of the newly processed ADCP data and ocean current measurements from MAK-1 and MAK-2 moorings. The surface layer profile is derived from the 7 and 3 months of ADCP data from MAK-1 and MAK-2, respectively, and is extrapolated through the rest of the deployment period using regression analyses: for the ADCP data deeper than 60 m to the current meter at 200 m (CM200) and for the shallower ADCP data to the zonal wind speeds in the Java Sea as measured by NSCAT and ERS-2 scatterometers.

[24] Persistent southward mean flow (the temporal average of the integrated velocity profile across the strait) with a maximum velocity within thermocline is observed for the entire mooring period. Similarly, the high-resolution global ocean model for the Earth simulator could mimic the observation results [*IPRC*, 2004]. After removing the mean flow, EOF analysis is applied to the integrated velocity profiles across the strait to obtain the vertical mode structure variability. The results indicate that only the first two modes are significant. Because the observed time series is less than 2 years, a cautionary note must be taken into account when interpreting the EOF results.

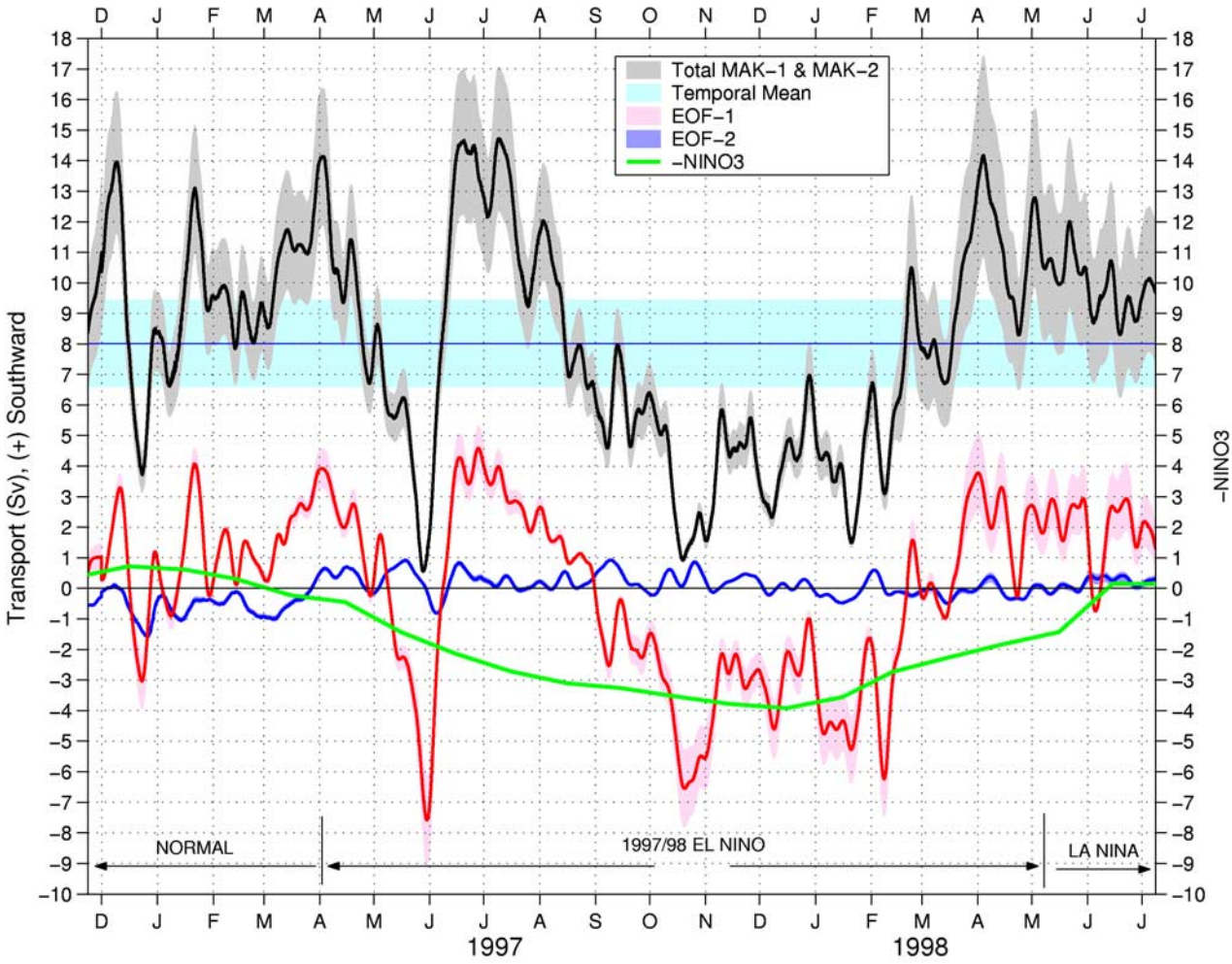

Figure 8. Depth-integrated transports with contributions of each mode and the ENSO phase as defined by NINO3 index. The total transport for the entire mooring record is 8.1 Sv, and that of the calendar 1997 is 7.9 Sv with standard deviations of 1.5 Sv and 1.2 Sv, respectively. Lesser transport (4.6 Sv) is observed during the peak of 1997/1998 El Niño from September 1997 to February 1998, compared to the rest of the mooring record.

[25] Though the time series is too short to conclude with assurance, we suggest that the first mode variability is a consequence of remote forcing, i.e., the 1997/1998 El Niño–Indian Dipole Mode event and Kelvin waves. This mode affects entire water column above the sill depth, and enhances the southward mean flow during the normal and La Niña conditions, but reduces the mean flow during the 1997/1998 El Niño. The second mode probably represents the seasonal effect of regional winds. Northward surface intensified flow is observed during the peak of northwest monsoon from December 1996 to February 1997. Northward flow, albeit weaker, is projected to occur during the El Niño period from December 1997 to February 1998. The southward flow in the top layer begins in April, marking the monsoon transition, reaching a maximum in June during southeast monsoon and decreasing during the monsoon transition in November.

[26] **Acknowledgments.** Analysis of the Arlindo and remote sensed data is derived from NSF grant OCE00-99152 and NASA grant JPLCIT 1228179. We gratefully acknowledge the fruitful comments from both anonymous reviewers. We also thank Tim Liu (NASA-JPL) for providing the NSCAT data. We thank Kevin Vranes for comments and discussion. Lamont-Doherty contribution 6655.

References

Burnett, W. H., V. M. Kamenkovich, G. L. Mellor, and A. L. Gordon (2000), The influence of the pressure head on the Indonesian Seas circulation, *Geophys. Res. Lett.*, *27*(15), 2273–2276.

Feng, M., and G. Meyers (2003), Interannual variability in the tropical Indian Ocean: A two-year time-scale of Indian Ocean dipole, *Deep Sea Res., Part II*, *50*, 2263–2284.

Ffield, A. L., K. Vranes, A. L. Gordon, R. D. Susanto, and S. L. Garzoli (2000), Temperature variability within Makassar Strait, *Geophys. Res. Lett.*, *27*(2), 237–240.

Gordon, A. L., and R. Fine (1996), Pathways of water between the Pacific and Indian oceans in the Indonesian seas, *Nature*, *379*, 146–149.

Gordon, A. L., and R. D. Susanto (1999), Makassar Strait transport: Initial estimate based on Arlindo results, *Mar. Technol. Soc. J.*, *32*, 34–45.

Gordon, A. L., R. D. Susanto, and A. L. Ffield (1999), Throughflow within Makassar Strait, *Geophys. Res. Lett.*, *26*(21), 3325–3328.

Gordon, A. L., R. D. Susanto, and K. Vranes (2003a), Cool Indonesian Throughflow as a consequence of restricted surface layer flow, *Nature*, *425*, 824–828.

Gordon, A. L., C. F. Giulivi, and A. G. Ilahude (2003b), Deep topographic barriers within the Indonesian Seas, *Deep Sea Res., Part II*, *50*, 2205–2228.

Hautala, S., J. Sprintall, J. T. Potemra, J. C. Chong, W. Pandoe, N. Bray, and A. Ilahude (2001), Velocity structure and transport of the Indonesian

Throughflow in the major straits restricting flow into the Indian Ocean, *J. Geophys. Res.*, *106*, 19,527–19,546.
International Pacific Research Center (IPRC) (2004), Global ocean modeling using the Earth simulator, *IPRC Clim.*, *3*, 16–18.
Murtugudde, R., J. P. McCreary Jr., and A. J. Busalacchi (2000), Oceanic processes associated with anomalous events in the Indian Ocean with relevance to 1997–1998, *J. Geophys. Res.*, *105*, 3295–3306.
Potemra, J., S. Hautala, and J. Sprintall (2003), Vertical structure of Indonesian throughflow in a large-scale model, *Deep Sea Res., Part II*, *50*, 2143–2161.
Saji, N. H., B. N. Goswami, P. N. Vinayachandran, and T. Yamagata (1999), A dipole mode in the tropical Indian Ocean, *Nature*, *401*, 360–363.
Smith, W. H. D., and T. Sandwell (1997), Global sea floor topography from satellite altimetry and ship depth soundings, *Science*, *277*, 1956–1962.
Sprintall, J., A. L. Gordon, R. Murtugudde, and R. D. Susanto (2000), A semiannual Indian Ocean forced Kelvin wave observed in the Indonesian seas in May 1997, *J. Geophys. Res*, *105*, 17,217–17,230.
Susanto, R. D., A. L. Gordon, J. Sprintall, and B. Herunadi (2000), Intraseasonal variability and tides in Makassar Strait, *Geophys. Res. Lett.*, *27*(10), 1499–1502.
Susanto, R. D., A. L. Gordon, and Q. Zheng (2001), Upwelling along the coasts of Java and Sumatra and its relation to ENSO, *Geophys. Res. Lett.*, *28*(8), 1599–1602.
Vranes, K., A. L. Gordon, and A. Ffield (2002), The heat transport of the Indonesian throughflow and implications for the Indian Ocean heat budget, *Deep Sea Res., Part II*, *49*, 1391–1410.
Wajsowicz, R. C. (1996), Flow of a western boundary current through multiple straits: An electrical circuit analogy for the Indonesian throughflow and archipelago, *J. Geophys. Res.*, *101*, 12,295–12,300.
Wajsowicz, R. C., A. L. Gordon, A. Ffield, and R. D. Susanto (2003), Estimating transport in Makassar Strait, *Deep Sea Res., Part II*, *50*, 2163–2181.
Waworuntu, J. M., S. L. Garzoli, and D. B. Olson (2001), Dynamics of Makassar Strait, *J. Mar. Res.*, *59*, 313–325.

A. L. Gordon and R. D. Susanto, Lamont-Doherty Earth Observatory of Columbia University, 61 Route 9W, 205 Oceanography, Palisades, NY 10964-8000, USA. (dwi@ldeo.columbia.edu)